ACS OMEGA

Article

Cite This: ACS Omega 2019, 4, 1410−1415

http://pubs.acs.org/journal/acsodf

# Glassy Carbon Electrodes Modified with Ordered Mesoporous Silica for the Electrochemical Detection of Cadmium Ions

Ana-Maria Sacara,[†] Federica Pitzalis,[‡] Andrea Salis,*[,‡] Graziella Liana Turdean,[†] and Liana Maria Muresan*[,†]

[†]Department of Chemical Engineering, "Babes-Bolyai" University, 11, Arany Janos Street, 40028 Cluj-Napoca, Romania

[‡]Dipartimento di Scienze Chimiche e Geologiche, Università degli Studi di Cagliari, CSGI, and CNBS, Cittadella Universitaria, SS 554 bivio Sestu, 09042, Monserrato, Cagliari, Italy

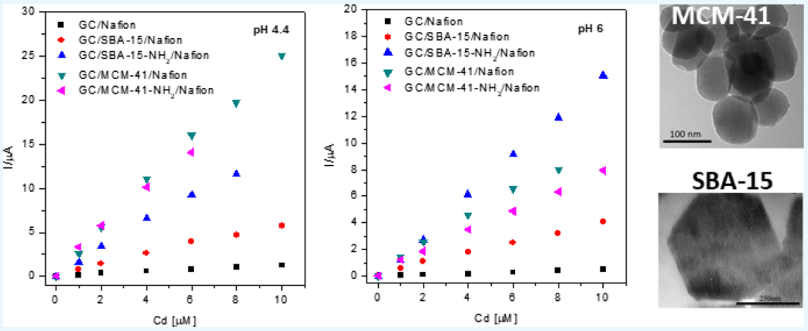


**ABSTRACT:** Four different samples of ordered mesoporous silica powders (MCM-41 and SBA-15) and amino-functionalized mesoporous silica (MCM-41-$NH_2$ and SBA-15-$NH_2$) were used to prepare modified glassy carbon electrodes coated with ion-exchange polymer Nafion to be used for the electrochemical detection of Cd(II). The mesoporous silica samples were characterized through transmission electron microscopy, small-angle X-ray scattering, and $N_2$-adsorption/desorption isotherms. The electrodes were characterized by using square wave anodic stripping voltammetry. The effect of pH and of the silica type on the electrodes' response was investigated. The influence of amino functional groups grafted on the silica surface toward Cd(II) ion detection was also examined. The detection limits determined with the new silica-modified electrodes [between 0.36 and 1.68 $\mu$M Cd(II)] are slightly higher than those reported in the literature, but they are lower than those stipulated in the European legislation [45 $\mu$M Cd(II)] and, consequently, the electrodes could be successfully used to detect Cd(II) in aqueous solutions.

## 1. INTRODUCTION

Cadmium ion detection is of great interest because of their long half-life and accumulation in tissues and organs, mainly in kidneys and liver.[1] Cd(II) is essentially a cumulative poison exhibiting carcinogenic activity, and for these reasons, the measurement of cadmium is important in clinical and toxicology laboratories. Electrochemical detection of Cd(II) has great potential for environmental monitoring of toxic metal ions because of the portability of electrodes and their excellent detection limits (DLs). The detection can be carried out by using mainly anodic stripping voltammetry with different modified electrodes: carbon paste electrodes modified with zirconium-phosphated silica,[1] diacetyldioxime,[2] zeolites,[3,4] carbon nanotubes,[5] conducting polymers,[6] and so forth; bismuth-modified carbon electrodes;[7−13] silica-modified electrodes;[14−17] and many others.[18,19]

Ordered mesoporous silica (OMS) materials have widely been investigated for several applications. Since their discovery in the 1990s,[20] they have been used for catalysis,[21,22] biocatalysis,[23−26] adsorption,[27,28] and as drug delivery carriers.[29−32] The main goal of these materials is due to their large specific surface area and highly uniform pore size. Despite their low conductivity, OMSs can be used for electrode material preparation because of their high adsorption capacity and large specific surface area, which could be advantageously exploited in the preconcentration of electroactive analytes before their electrochemical detection.[33] As nonconductors, OMSs do not contribute to the charging current when they are used as electrode modifiers, thus leading to low background.[34] On the other hand, silica-based mesoporous materials can be grafted with a large variety of organic functionalities, which prevent their leaching from the electrode surface, leading to a good stability of the electrodes, or facilitate the electrode reaction. In this context, we recently compared SBA-15 and MCM-41 as matrices for the modification of glassy carbon (GC) electrodes for the voltammetric detection of malachite green.[35]

**Received:** November 27, 2018
**Accepted:** January 4, 2019
**Published:** January 16, 2019






DOI: 10.1021/acsomega.8b03305
ACS Omega 2019, 4, 1410−1415

In this work, four different OMS powders belonging to two different classes (MCM-41 and SBA-15) were used to prepare modified GC electrodes coated with Nafion to be used for the electrochemical detection of Cd(II) ions. The influence of the silica type and their characteristics on the electrochemical response of the modified electrodes was investigated by using square wave anodic stripping voltammetry (SWASV) at two pH values (6 and 4.4). In order to better understand the differences between the electrochemical behavior of the electrodes fabricated with different types of silica, the role of amino functional groups grafted on the silica surface in the Cd(II) ion detection was also examined.

## 2. RESULTS AND DISCUSSION

**2.1. Synthesis and Characterization of OMS Samples.** The synthesized mesoporous silica materials, MCM-41 and SBA-15, were functionalized with aminopropyl-triethoxysilane to obtain the aminopropyl-functionalized MCM-41-$NH_2$ and SBA-15-$NH_2$ samples. The four samples were then characterized through $N_2$-physisorption isotherms, small-angle X-ray scattering (SAXS), and transmission electron microscopy (TEM). The $N_2$-physisorption isotherms of MCM-41, SBA-15, and the relative amino-functionalized samples are shown in Figure 1A. MCM-41 and MCM-4-$NH_2$ (type IV) isotherms

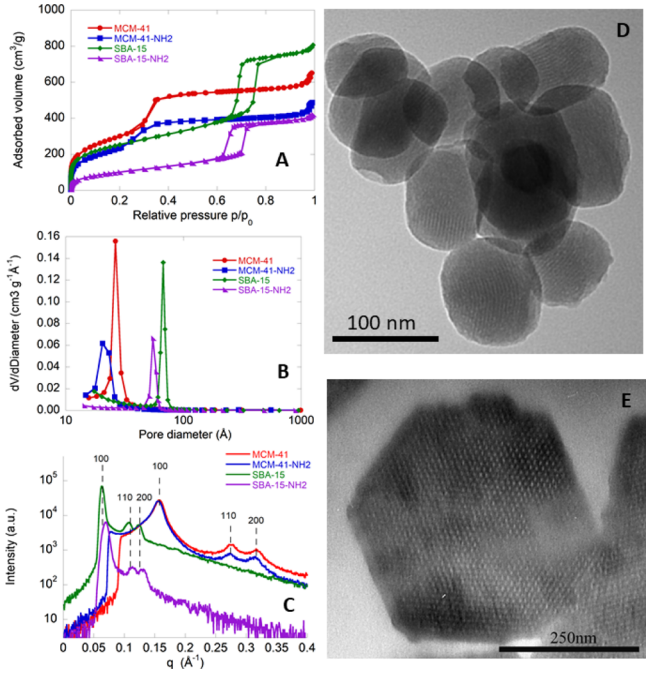


**Figure 1.** Characterization of MCM-41, MCM-41-$NH_2$, SBA-15, and SBA-15-$NH_2$ OMS samples. (A) $N_2$-physisorption isotherms, (B) pore size distributions, (C) SAXS patterns, and (D,E) TEM images.

show an increase of $N_2$ volume adsorption at a relative pressure between 0.2 and 0.4 $p/p_0$. The isotherms are reversible and do not show any appreciable hysteresis loop. SBA-15 and SBA-15-$NH_2$ also exhibit a type IV isotherm, with a sharp increase of $N_2$ volume adsorption at the relative pressure of $p/p_0$ = 0.6−0.7, as expected considering their wider pores with respect to those of MCM-41-based materials. In this case, a H1 hysteresis cycle due to the capillary condensation of nitrogen into the mesopores occurs. The SBA-15-$NH_2$ curve is shifted toward low adsorbed nitrogen volumes with respect to that of SBA-15. Indeed, the functionalization step with 3-aminopropyltriethoxysilane (APTES) brings to a decrease of the pore volume and of the pore size. Figure 1B shows the pore size distributions for the four mesoporous silica samples. The obtained values of the surface area, pore volume, and the maximum of the pore size distribution are all reported in Table 1. The SAXS patterns of

**Table 1. Characteristics of the Various Mesoporous Silica Samples**

| sample | $^aS_{BET}$ ($m^2/g$) | $^bd_{Des,BJH}$ (Å) | $^cV_{pDes,BJH}$ ($cm^3/g$) | $^da$ (Å) |
|---|---|---|---|---|
| MCM-41 | 1061 | 27 | 1.41 | 45 |
| MCM-41-$NH_2$ | 894 | 21 | 0.98 | 46 |
| SBA-15 | 880 | 67 | 1.25 | 117 |
| SBA-15-$NH_2$ | 373 | 55 | 0.65 | 119 |

[a]Specific surface area calculated by the BET method. [b]Pore diameter calculated by applying the BJH method to the data of the desorption branch. [c]Cumulative pore volume. [d]Lattice parameter obtained by SAXS.

all mesoporous silica samples, shown in Figure 1C, have the typical pattern of hexagonal structures, that is an intense peak because of the reflection of the (100) plane and two weaker peaks because of the reflection of the (110) and (200) planes, respectively. The peaks for SBA-15 and SBA-15-$NH_2$ samples fall at lower q values than those of MCM-41 and MCM-41-$NH_2$ as a result of larger lattice parameter ($a$) values (Table 1). TEM micrographs confirm that both MCM-41 (Figure 1D) and SBA-15 (Figure 1E) are constituted by parallel channels organized according to an ordered hexagonal array. Moreover, TEM images clearly show that MCM-41 particles are quasispherical with a diameter of around 80−100 nm, whereas SBA-15 particles have a hexagonal shape and a size of about 500 nm.

**2.2. Influence of pH and of Silica Type.** The effect of the nature of the silica types on the voltammetric response of the silica-modified electrodes toward Cd(II) detection was investigated at two pH values (4.4 and 6). By anodic stripping voltammetry (SWASV), the analyte of interest is electrodeposited on the working electrode during a reduction step and then oxidized from the electrode during the stripping step, the resulting current being measured.[36] Thus, for Cd(II) detection by SWASV, a first step of preconcentration was operated at −1.3 V versus Ag/AgCl,$KCl_{sat}$ during an accumulation time of 120 s, which was chosen after preliminary experiments as the optimal deposition time. The performance of each silica type in the same experimental conditions was evaluated and discussed. The SWASV responses are presented in Figure 2.

It can be observed that at both pH values, the peak currents increase significantly at silica-modified electrodes. This is certainly due to the increase of the electrode-specific surface area in the presence of silica and to its ability to adsorb electroactive species during the accumulation step. Additionally, a broadening of the peaks is noticed, especially at higher concentrations of Cd(II) (Figure 3). A possible explanation could be a sluggishness of the electrode kinetics or interactions between adsorbed species that may be expected to become more significant as the surface coverage increases.[37] There is also a slight difference in oxidation potential between electrodes at the two pH values illustrated in Table 2 for SBA-15 and SBA-15-$NH_2$-modified GC electrodes, suggesting


DOI: 10.1021/acsomega.8b03305
ACS Omega 2019, 4, 1410−1415

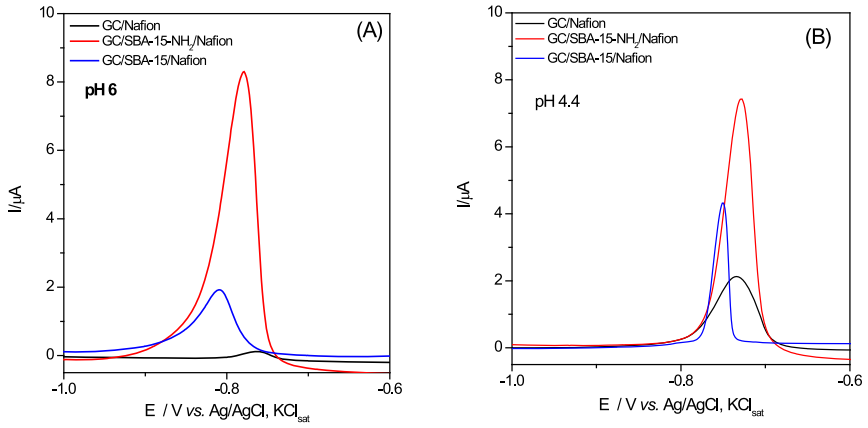


**Figure 2.** SWASV measurements for GC/Nafion and GC/silica/Nafion electrodes in 4 $\mu$M Cd(II) solution at pH 6 (A) and 4.4 (B). Experimental conditions: electrolyte, 0.1 M phosphate buffer; starting potential, −1.3 V vs Ag/AgCl, $KCl_{sat}$; frequency, 25 Hz; amplitude, 0.005 V; step potential, 0.004 V; deposition potential −1.3 V vs Ag/AgCl, $KCl_{sat}$; deposition time, 120 s; equilibration, 10 s; electrode conditioning, 0 V vs Ag/AgCl, $KCl_{sat}$; duration, 60 s, deoxygenation using Ar for 5 min before measurements and 30 s between each measurement.

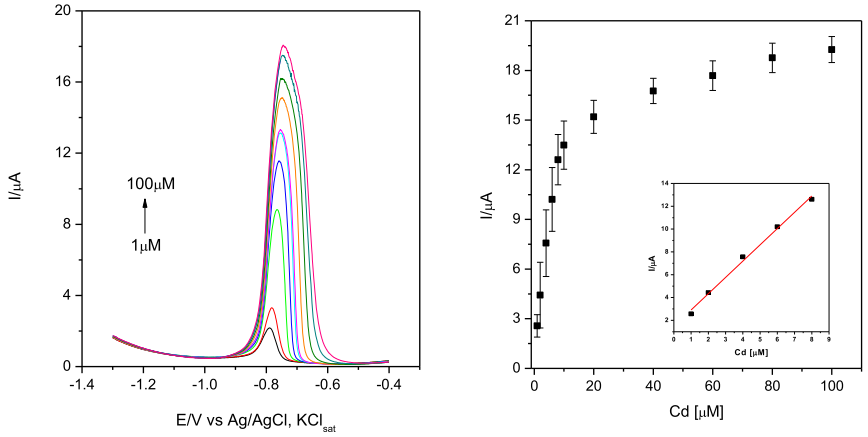


**Figure 3.** SWASV measurements for Cd(II) detection at GC/SBA-15-$NH_2$/Nafion-modified electrodes in phosphate buffer of pH 6 (left) and the corresponding calibration curves (right). Inset: linear region of the polarization curve. Experimental conditions: electrolyte, 0.1 M phosphate buffer; starting potential, −1.3 V vs Ag/AgCl, $KCl_{sat}$; frequency, 25 Hz; amplitude, 0.005 V; step potential, 0.004 V; deposition potential −1.3 V vs Ag/AgCl, $KCl_{sat}$; deposition time, 120 s; equilibration, 10 s; electrode conditioning, 0 V vs Ag/AgCl, $KCl_{sat}$; duration, 60 s, deoxygenation using Ar for 5 min before measurements and 30 s between each measurement. The error bars correspond to the mean of three successive measurements with three different electrodes.

that at more acidic pH values the electron transfer takes place more easily.

**Table 2. Oxidation Potentials for Cd at Various Silica-Modified Electrodes at pH 4.4 and 6**

| | *E*/V vs Ag/AgCl, $KCl_{sat}$ | |
|---|---|---|
| electrode types | pH 4.4 | pH 6 |
| GC/Nafion | −0.734 | −0.760 |
| GC/SBA-15/Nafion | −0.751 | −0.809 |
| GC/SBA-15-$NH_2$/Nafion | −0.728 | −0.778 |

As expected, the height of the oxidation peak of Cd increases with its concentration, leading to a calibration curve where a linear domain at low concentration of Cd(II) can be identified (see as example Figure 3 for the GC/SBA-15-$NH_2$/Nafion electrodes at pH 6).

**2.3. Calibration Curves and Electroanalytical Parameters.** The calibration curves corresponding to all modified electrodes at the beginning of their linear domain are presented in Figure 4. In fact, the different modified electrodes showed different linearity ranges, which depend on both the OMS sample and the operational pH, as reported in Table 3. Table 3 also reports other electroanalytical parameters as, for example, the DLs, which were calculated for a signal-to-noise ratio of 3, using the formula: DL = $\frac{3SD}{slope}$, where the slope and standard deviation (SD) correspond to the parameters of the fitting equation.

All silica powders have a good impact on the detection of metal ions because of their adsorption properties. At both tested pH values, the DL is smaller for GC/SBA-15-$NH_2$/Nafion than for GC/SBA-15/Nafion electrodes, which suggests a better efficiency to detect Cd(II) of the first ones. The effect is more pronounced at pH 6. It is probable that amino groups bind metal ions, increasing their concentration at the interface[38] and hence lowering the DLs.

The effect of pH is less remarkable in the case of GC/MCM-41-$NH_2$/Nafion and GC/MCM-41/Nafion electrodes. A decrease of DL at the GC/MCM-41-$NH_2$/Nafion electrode is noticed at pH 6, but no significant differences of sensitivities and DLs were noticed between MCM-41 and MCM-41-$NH_2$



DOI: 10.1021/acsomega.8b03305
ACS Omega 2019, 4, 1410−1415

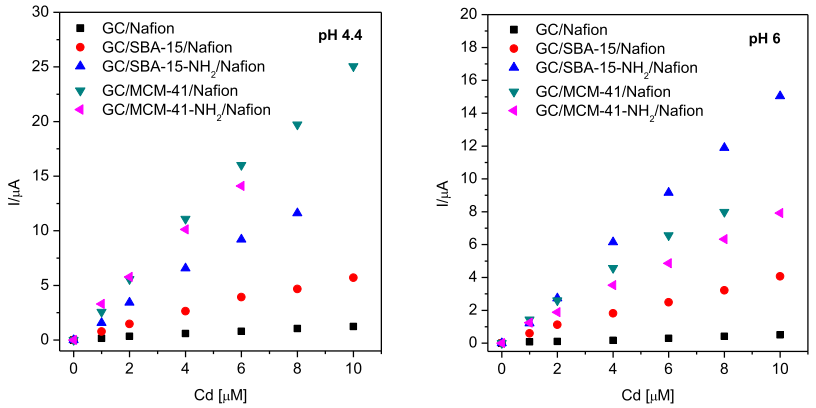


**Figure 4.** Calibration curves for Cd(II) detection at different silica-modified GC electrodes. For experimental conditions, see Figure 3.

**Table 3. Electroanalytical Parameters for Silica-Modified GC Electrodes of Different Types. For Experimental Conditions, See Figure 3**

| | sensitivity (A/M) | | DL ($\mu$M) | | linear domain ($\mu$M) | | $R^2$/no. of points | |
|---|---|---|---|---|---|---|---|---|
| electrode | pH 6 | pH 4.4 | pH 6 | pH 4.4 | pH 6 | pH 4.4 | pH 6 | pH 4.4 |
| GC/Nafion | 0.013 ± 0.001 | 0.165 ± 0.049 | 4.79 | 4.14 | 0−100 | 0−10 | 0.9987/12 | 0.9914/7 |
| GC/SBA-15/Nafion | 0.377 ± 0.007 | 0.564 ± 0.023 | 0.97 | 1.10 | 0−20 | 0−10 | 0.9979/8 | 0.9920/7 |
| GC/SBA-15-$NH_2$/Nafion | 1.520 ± 0.020 | 1.462 ± 0.052 | 0.36 | 0.73 | 0−10 | 0−8 | 0.9991/7 | 0.9950/6 |
| GC/MCM-41/Nafion | 0.992 ± 0.047 | 2.487 ± 0.063 | 0.97 | 0.70 | 0−8 | 0−10 | 0.9912/6 | 0.9968/7 |
| GC/MCM-41-$NH_2$/Nafion | 0.765 ± 0.020 | 2.300 ± 0.121 | 0.71 | 0.76 | 0−10 | 0−6 | 0.9909/7 | 0.9901/5 |

at pH 4.4. It should also be mentioned that despite its smaller specific surface area, the SBA-15-$NH_2$ sample was proven to be more performing than MCM-41-$NH_2$ in which the DL is concerned. From data listed in Table 3, we also observe that the electrode sensitivity depends both on the type of silica and on the solution pH. SBA-15-$NH_2$ has a higher sensitivity at both pHs than the unmodified SBA-15 (approximately four times higher at pH 6 and three times higher at pH 4.4). This could be due to the fact that at pH 6, the coordination of Cd(II) by amino groups is the driving mechanism and, at pH 4.4, the protonation of $-NH_2$ groups may decrease cadmium coordination. Even if the DL values are higher than those reported by other authors,[1] the proposed electrodes could be successfully used to determine Cd(II) in industrial sources of heavy metals, such as industrial wastewater and sewage sludge, where the concentration of Cd(II) could be relatively high.[39]

**2.4. Reproducibility and Repeatability.** Reproducibility of the GC/SBA-15-$NH_2$/Nafion electrode was assessed at pH 6 on four consecutive measurements of 10 $\mu$M solution of Cd(II) and the mean value of the obtained peak current was $1.828 \times 10^{-5}$ A, with a relative SD (RSD) of 5.87%. Repeatability was tested on three different electrodes in the same 4 $\mu$M Cd(II) solution and the mean value of the obtained peak current was $6.304 \times 10^{-6}$ A, with an RSD of 1.90%.

**2.5. Real Sample Analysis.** Determination of Cd(II) concentration was performed by SWASV, with the GC/SBA-15-$NH_2$/Nafion electrode, on a natural underground water sample, collected by drilling from a site situated in Salaj district (Romania). The peak height value, measured three times (with the same electrode) and mediated, was interpolated on a premade calibration curve, and the concentration was determined. The calibration curve was done on a 0.5−10 $\mu$M Cd(II) concentration range, at pH 6 (considering that the pH of the water sample was 5.5, determined before the SWASV measurement), under the same working conditions as all SWASV measurements before (for experimental conditions, see Figure 3).

The performances of the proposed electrochemical method of detection for Cd(II) were compared against the standard F-AAS method, with results presented in Table 4. As observed, the agreement between the results obtained by the two methods was very good. By using the silica-modified electrode, the Cd(II) concentration was found to be 98.09% from the standard method.

**Table 4. Comparison between Electrochemical and F-AAS Methods for Cd (II) Detection**

| Cd(II)/$\mu$M | | |
|---|---|---|
| GC/SBA-15-$NH_2$/Nafion | F-AAS | recovery (%) |
| 9.25 ± 0.16 | 9.43 ± 0.09 | 98.9, 2.28 |

## 3. CONCLUSIONS

Four different mesoporous silica powders were used to prepare modified GC electrodes coated with ion-exchange polymer Nafion to be used for the electrochemical detection of Cd(II). The silica powders have a good impact on the detection of metal ions because of their adsorption properties. The large specific surface area of silica powders certainly plays a key role in their performance, but in some cases, the most important is the effect of the $-NH_2$ groups, which have a beneficial influence, most probably because of the complexation possibility of cadmium ions. Other characteristics could also be taken into consideration. The electrodes' analytical performances increase in the series: GC/SBA-15/Nafion (pH 4.4 and 6) ≅ GC/MCM-41/Nafion (pH 6) < GC/MCM-41/Nafion (pH 4.4) ≅ GC/MCM-41-$NH_2$/Nafion (pH 4.4 and 6) ≅ GC/SBA-15-$NH_2$/Nafion (pH 4.4) < GC/SBA-15-$NH_2$/



DOI: 10.1021/acsomega.8b03305
ACS Omega 2019, 4, 1410−1415

Nafion (pH 6). Even though the DL values determined with the new silica-modified electrodes are slightly higher than those reported in the literature, the electrodes are easy to prepare and could successfully be used to detect Cd(II) in real aqueous solutions.

## 4. EXPERIMENTAL SECTION

**4.1. Chemicals.** Tetraethoxysilane (98%), hexadecyltrimethylammonium bromide (CTAB, >99%), Pluronic copolymer 123 ($EO_{20}$-$PO_{70}EO_{20}$), sodium hydroxide, anhydrous toluene (99.8%), APTES (>98%), triethylamine (>99%), and hydrochloric acid (37%) were purchased from Sigma-Aldrich (Milan). A 0.1 M phosphate buffer solution was prepared from $NaH_2PO4$ and $Na_2HPO_4$ (Merck, Darmstadt, Germany). The pH of the buffer solutions was adjusted to the desired values by adding $H_3PO_4$ solution (Merck, Darmstadt, Germany). Sodium dodecyl sulfate (SDS) and Nafion (5% in ethanol) solution were purchased from Sigma-Aldrich. Distilled water was used for preparing all solutions. All reagents were of analytical degree and were used without further purification.

**4.2. Synthesis, Functionalization, and Characterization of OMS Samples.** MCM-41 and SBA-15 samples were synthesized according to the procedures reported in refs 39 and 40, respectively. The organic surfactants, either CTAB or Pluronic 123, were removed by calcination at 550 °C for 5 h. The functionalized MCM-41-$NH_2$ (SBA-15-$NH_2$) was prepared by adding 1 mL of APTES to a suspension of 1 g of MCM-41 (SBA-15) in 30 mL of anhydrous toluene. The mixture was heated under reflux for 15 h. The resulting solid was filtered and washed with acetone and dried overnight under vacuum at room temperature.[31] Textural analysis was carried out on an ASAP 2020 instrument by determining the $N_2$-adsorption/-desorption isotherm at 77 K. Before analysis, MCM-41 and SBA-15 samples were heated at 250 °C at a rate of 1 °C/min under vacuum for 12 h, whereas MCM-41-$NH_2$ and SBA-15-$NH_2$ were heated at 110 °C at the rate of 1 °C/min under vacuum for 24 h. The Brunauer−Emmett−Teller (BET)[41] and Barrett−Joyner−Halenda (BJH)[42] methods were used to calculate the specific surface area and pore size distribution (from the desorption branch), respectively. SAXS patterns were recorded by means of a S3-MICRO SWAXS camera system (HECUS X-ray Systems, Graz, Austria). Thin-walled 2 mm glass capillaries were filled with the sample for the scattering experiments and analyzed under the same conditions reported in ref 26. TEM images were obtained on a JEOL 100S microscope, and finely ground samples were placed directly onto formvar-coated electron microscopy nickel grids.

**4.3. Preparation of GC/Silica/Nafion-Modified Electrodes.** Before conducting any measurements, the GC working electrode was cleaned thoroughly on a piece of felt with $\gamma$-alumina paste until mirror-like shine was obtained. It was subsequently washed in an ultrasound bath with distilled water to rinse off any trace of alumina. Mesoporous silica suspensions were stabilized by means of sodium dodecyl sulfate (SDS),[35] which allowed to obtain a homogeneous suspension and to prevent precipitation and aggregation of silica particles. The suspensions (5 $\mu$L) were applied by drop-casting on the electrode's active surface and dried. To improve stability, a coating with 5 $\mu$L of 0.5% Nafion was created using the same method.

**4.4. Electrochemical Measurements.** All electrochemical experiments were performed on a Metrohm Autolab PGSTAT 302N, electrochemical workstation (Eco Chemie, The Netherlands). A three-electrode system was used, composed of an Ag/AgCl, a $KCl_{sat}$ reference electrode, a platinum wire counter electrode, and a GC working electrode, bare or modified. The electrolyte solution was 0.1 M phosphate buffer (adjusted at pH 4.4 and 6). The two pH values were selected, according to literature data,[43,44] in order to find the best working conditions, taking into account that the behavior of $-NH_2$-containing silica powders is influenced by the acidity of the buffer solution. pH values above 6.0 can decrease the electrode signal noticeably, as Cd(II) ions would precipitate as hydroxide sediments.[19] All experiments were performed at room temperature. Square wave voltammetry measurements were performed using a preconcentration time of 120 s at −1.3 V, followed by a potential stripping from −1.3 to −0.4 V, with a frequency of 25 Hz.

**4.5. Real Sample Analysis.** The real underground water sample was analyzed by F-AAS (atomic absorption spectroscopy in flame) with a contrAA 800 F atomic absorption spectrometer. The analysis was repeated three times, and the results were mediated for comparison with the electrochemical method.

## AUTHOR INFORMATION


### Corresponding Authors

*E-mail: asalis@unica.it (A.S.).
*E-mail: limur@chem.ubbcluj.ro (L.M.M.).

### ORCID

Andrea Salis: 0000-0001-5746-2693


### Notes

The authors declare no competing financial interest.

## ACKNOWLEDGMENTS

FIR 2017−2018, Fondazione di Sardegna/Regione Autonoma della Sardegna (CUP F72F16003070002), and FFABR 2017 (MIUR) are acknowledged for financial support. Dr. M. Piludu is thanked for the TEM images of mesoporous silica samples. Project PN III—TRADE-IT—PCCDI no. 84/2018 financed by the UEFISCDI, Romania, is also acknowledged.

## REFERENCES


(1) Shams, E.; Torabi, R. Determination of Nanomolar Concentrations of Cadmium by Anodic-Stripping Voltammetry at a Carbon Paste Electrode Modified with Zirconium Phosphated Amorphous Silica. *Sens. Actuators, B* **2006**, *117*, 86−92.

(2) Hu, C.; Wu, K.; Dai, X.; Hu, S. Simultaneous Determination of Lead(II) and Cadmium(II) at a Diacetyldioxime Modified Carbon Paste Electrode by Differential Pulse Stripping Voltammetry. *Talanta* **2003**, *60*, 17−24.

(3) Senthilkumar, S.; Saraswathi, R. Electrochemical Sensing of Cadmium and Lead Ions at Zeolite-Modified Electrodes: Optimization and Field Measurements. *Sens. Actuators, B* **2009**, *141*, 65−75.

(4) Cao, L.; Jia, J.; Wang, Z. Sensitive Determination of Cd and Pb by Differential Pulse Stripping Voltammetry with in Situ Bismuth-Modified Zeolite Doped Carbon Paste Electrodes. *Electrochim. Acta* **2008**, *53*, 2177−2182.

(5) Tarley, C. R. T.; Santos, V. S.; Baêta, B. E. L.; Pereira, A. C.; Kubota, L. T. Simultaneous Determination of Zinc, Cadmium and Lead in Environmental Water Samples by Potentiometric Stripping Analysis (PSA) Using Multiwalled Carbon Nanotube Electrode. *J. Hazard. Mater.* **2009**, *169*, 256−262.

(6) Somerset, V.; Iwuoha, E.; Hernandez, L. Stripping Voltammetric Measurement of Trace Metal Ions at Screen-Printed Carbon and Carbon Paste Electrodes. *Procedia Chem.* **2009**, *1*, 1279−1282.




DOI: 10.1021/acsomega.8b03305
*ACS Omega* 2019, 4, 1410−1415

(7) Luo, L.; Wang, X.; Ding, Y.; Li, Q.; Jia, J.; Deng, D. Voltammetric determination of $Pb^{2+}$ and $Cd^{2+}$ with montmorillonite-bismuth-carbon electrodes. *Appl. Clay Sci.* **2010**, *50*, 154−157.
(8) Zhu, L.; Xu, L.; Huang, B.; Jia, N.; Tan, L.; Yao, S. Simultaneous Determination of Cd(II) and Pb(II) Using Square Wave Anodic Stripping Voltammetry at a Gold Nanoparticle-Graphene-Cysteine Composite Modified Bismuth Film Electrode. *Electrochim. Acta* **2014**, *115*, 471−477.
(9) Xu, H.; Zeng, L.; Huang, D.; Xian, Y.; Jin, L. A Nafion-Coated Bismuth Film Electrode for the Determination of Heavy Metals in Vegetable Using Differential Pulse Anodic Stripping Voltammetry: An Alternative to Mercury-Based Electrodes. *Food Chem.* **2008**, *109*, 834−839.
(10) Charalambous, A.; Economou, A. A Study on the Utility of Bismuth-Film Electrodes for the Determination of In(III) in the Presence of Pb(II) and Cd(II) by Square Wave Anodic Stripping Voltammetry. *Anal. Chim. Acta* **2005**, *547*, 53−58.
(11) Li, J.; Guo, S.; Zhai, Y.; Wang, E. High-Sensitivity Determination of Lead and Cadmium Based on the Nafion-Graphene Composite Film. *Anal. Chim. Acta* **2009**, *649*, 196−201.
(12) Rutyna, I.; Korolczuk, M. Determination of lead and cadmium by anodic stripping voltammetry at bismuth film electrodes following double deposition and stripping steps. *Sens. Actuators, B* **2014**, *204*, 136−141.
(13) Yi, W. J.; Li, Y.; Ran, G.; Luo, H. Q.; Li, N. B. Determination of cadmium(II) by square wave anodic stripping voltammetry using bismuth-antimony film electrode. *Sens. Actuators, B* **2012**, *166−167*, 544−548.
(14) Yang, D.; Wang, L.; Chen, Z.; Megharaj, M.; Naidu, R. Voltammetric Determination of Lead (II) and Cadmium (II) Using a Bismuth Film Electrode Modified with Mesoporous Silica Nanoparticles. *Electrochim. Acta* **2014**, *132*, 223−229.
(15) Yantasee, W.; Charnhattakorn, B.; Fryxell, G. E.; Lin, Y.; Timchalk, C.; Addleman, R. S. Detection of Cd, Pb, and Cu in Non-Pretreated Natural Waters and Urine with Thiol Functionalized Mesoporous Silica and Nafion Composite Electrodes. *Anal. Chim. Acta* **2008**, *620*, 55−63.
(16) Cheng, B.; Zhou, L.; Lu, L.; Liu, J.; Dong, X.; Xi, F.; Chen, P. Simultaneous Label-Free and Pretreatment-Free Detection of Heavy Metal Ions in Complex Samples Using Electrodes Decorated with Vertically Ordered Silica Nanochannels. *Sens. Actuators, B* **2018**, *259*, 364−371.
(17) Song, Y.; Jiang, H.; Bi, H.; Zhong, G.; Chen, J.; Wu, Y.; Wei, W. Multifunctional Bismuth Oxychloride/Mesoporous Silica Composites for Photocatalysis, Antibacterial Test, and Simultaneous Stripping Analysis of Heavy Metals. *ACS Omega* **2018**, *3*, 973−981.
(18) Dutta, S.; Strack, G.; Kurup, P. Gold nanostar electrodes for heavy metal detection. *Sens. Actuators, B* **2019**, *281*, 383−391.
(19) Dahaghin, Z.; Kilmartin, P. A.; Mousavi, H. Z. Determination of cadmium(II) using a glassy carbon electrode modified with a Cd-ion imprinted polymer. *J. Electroanal. Chem.* **2018**, *810*, 185−190.
(20) Kresge, C. T.; Leonowicz, M. E.; Roth, W. J.; Vartuli, J. C.; Beck, J. S. Ordered Mesoporous Molecular Sieves Synthesized by a Liquid-Crystal Template Mechanism. *Nature* **1992**, *359*, 710−712.
(21) Usai, E. M.; Sini, M. F.; Meloni, D.; Solinas, V.; Salis, A. Sulfonic Acid-Functionalized Mesoporous Silicas: Microcalorimetric Characterization and Catalytic Performance toward Biodiesel Synthesis. *Microporous Mesoporous Mater.* **2013**, *179*, 54−62.
(22) El Kadib, A.; Finiels, A.; Brunel, D. Sulfonic Acid Functionalised Ordered Mesoporous Materials as Catalysts for Fine Chemical Synthesis. *Chem. Commun.* **2013**, *49*, 9073−9076.
(23) Hartmann, M.; Kostrov, X. Immobilization of enzymes on porous silicas—benefits and challenges. *Chem. Soc. Rev.* **2013**, *42*, 6277−6289.
(24) Magner, E. Immobilisation of Enzymes on Mesoporous Silicate Materials. *Chem. Soc. Rev.* **2013**, *42*, 6213.
(25) Bolivar, J. M.; Eisl, I.; Nidetzky, B. Advanced Characterization of Immobilized Enzymes as Heterogeneous Biocatalysts. *Catal. Today* **2015**, *259*, 66−80.
(26) Pitzalis, F.; Monduzzi, M.; Salis, A. A Bienzymatic Biocatalyst Constituted by Glucose Oxidase and Horseradish Peroxidase Immobilized on Ordered Mesoporous Silica. *Microporous Mesoporous Mater.* **2017**, *241*, 145−154.
(27) Cugia, F.; Sedda, S.; Pitzalis, F.; Parsons, D. F.; Monduzzi, M.; Salis, A. Are Specific Buffer Effects the New Frontier of Hofmeister Phenomena? Insights from Lysozyme Adsorption on Ordered Mesoporous Silica. *RSC Adv.* **2016**, *6*, 94617−94621.
(28) Salis, A.; Medda, L.; Cugia, F.; Monduzzi, M. Effect of Electrolytes on Proteins Physisorption on Ordered Mesoporous Silica Materials. *Colloids Surf., B* **2016**, *137*, 77−90.
(29) Nairi, V.; Medda, L.; Monduzzi, M.; Salis, A. Adsorption and Release of Ampicillin Antibiotic from Ordered Mesoporous Silica. *J. Colloid Interface Sci.* **2017**, *497*, 217−225.
(30) Nairi, V.; Magnolia, S.; Piludu, M.; Nieddu, M.; Caria, C. A.; Sogos, V.; Vallet-Regì, M.; Monduzzi, M.; Salis, A. Mesoporous Silica Nanoparticles Functionalized with Hyaluronic Acid. Effect of the Biopolymer Chain Length on Cell Internalization. *Colloids Surf., B* **2018**, *168*, 50−59.
(31) Salis, A.; Fanti, M.; Medda, L.; Nairi, V.; Cugia, F.; Piludu, M.; Sogos, V.; Monduzzi, M. Mesoporous Silica Nanoparticles Functionalized with Hyaluronic Acid and Chitosan Biopolymers. Effect of Functionalization on Cell Internalization. *ACS Biomater. Sci. Eng.* **2016**, *2*, 741−751.
(32) Nairi, V.; Medda, S.; Piludu, M.; Casula, M. F.; Vallet-Regì, M.; Monduzzi, M.; Salis, A. Interactions between Bovine Serum Albumin and Mesoporous Silica Nanoparticles Functionalized with Biopolymers. *Chem. Eng. J.* **2018**, *340*, 42−50.
(33) Walcarius, A. Analytical Applications of Silica-Modified Electrodes—A Comprehensive Review. *Electroanalysis* **1999**, *10*, 1217−1235.
(34) Cui, L.; Wu, J.; Ju, H. Electrochemical Sensing of Heavy Metal Ions with Inorganic, Organic and Bio-Materials. *Biosens. Bioelectron.* **2015**, *63*, 276−286.
(35) Sacara, A. M.; Nairi, V.; Salis, A.; Turdean, G. L.; Muresan, L. M. Silica-Modified Electrodes for Electrochemical Detection of Malachite Green. *Electroanalysis* **2017**, *29*, 2602−2609.
(36) Copeland, T. R.; Skogerboe, R. K. Anodic Stripping Voltammetry. *Anal. Chem.* **1974**, *46*, 1257A−1268A.
(37) Honeychurch, M. J.; Ridd, M. J. Derivative Chronopotentiometric Stripping Analysis of Insulin. *Electroanalysis* **1996**, *8*, 49−54.
(38) Dai, X.; Qiu, F.; Zhou, X.; Long, Y.; Li, W.; Tu, Y. Amino-Functionalized Mesoporous Silica Modified Glassy Carbon Electrode for Ultra-Trace Copper(II) Determination. *Anal. Chim. Acta* **2014**, *848*, 25−31.
(39) Slowing, I. I.; Trewyn, B. G.; Lin, V. S.-Y. Mesoporous Silica Nanoparticles for Intracellular Delivery of Membrane-Impermeable Proteins. *J. Am. Chem. Soc.* **2007**, *129*, 8845−8849.
(40) Zhao, D.; Feng, J.; Huo, Q.; Melosh, N.; Fredrickson, G. H.; Chmelka, B. F.; Stucky, G. D. Triblock Copolymer Syntheses of Mesoporous Silica with Periodic 50 to 300 Angstrom Pores. *Science* **1998**, *279*, 548−552.
(41) Brunauer, S.; Emmett, P. H.; Teller, E. Adsorption of Gases in Multimolecular Layers. *J. Am. Chem. Soc.* **1938**, *60*, 309−319.
(42) Barrett, E. P.; Joyner, L. G.; Halenda, P. P. The Determination of Pore Volume and Area Distributions in Porous Substances. I. Computations from Nitrogen Isotherms. *J. Am. Chem. Soc.* **1951**, *73*, 373−380.
(43) Jiang, L.; Wang, Y.; Ding, J.; Lou, T.; Qin, W. An ionophore-Nafion modified bismuth electrode for the analysis of cadmium(II). *Electrochem. Commun.* **2010**, *12*, 202−205.
(44) Ismail, A.; Kawde, A.; Muraza, O.; Sanhoob, M. A.; Al-Betar, A. R. Lanthanum-impregnated zeolite modified carbon paste electrode for determination of Cadmium (II). *Microporous Mesoporous Mater.* **2016**, *225*, 164−173.



DOI: 10.1021/acsomega.8b03305
*ACS Omega* 2019, 4, 1410−1415